

1 **Microscopic observation of morphological changes in cerebral arteries and veins in hyperacute phase**
2 **after experimental subarachnoid hemorrhage: an *in vivo* analysis**

3 **Running title:** Arterial instability in hyperacute SAH

4

5 [†]Kana **Fujimori**¹, [†]Sosho **Kajiwara**¹, *Yu **Hasegawa**^{1,2}, Hiroki **Uchikawa**³, Motohiro **Morioka**¹

6 [†]These authors contributed equally to this work.

7

8 ¹Department of Neurosurgery, Kurume University School of Medicine, Fukuoka, Japan

9 ²Department of Pharmaceutical Sciences, School of Pharmacy at Fukuoka, International University of
10 Health and Welfare, Fukuoka, Japan

11 ³Department of Neurosurgery, Kumamoto University School of Medicine, Kumamoto, Japan

12

13 Address correspondence and reprint requests to:

14 Yu Hasegawa, MD, PhD

15 Department of Pharmaceutical Sciences, School of Pharmacy at Fukuoka, International University of
16 Health and Welfare, 137-1, Enokizu, Okawa, Fukuoka, 8318501, Japan

17 Tel: 81-944-89-2000/Fax: 81-944-89-2001

18 E-mail: yhasegawa@iuhw.ac.jp

19

20

21 **Abstract**

22 This observational study examined morphological changes in superficial cerebral arteries and veins, which
23 were correlated with increased intracranial pressure (ICP)-dependent and -independent hypoperfusion in
24 hyperacute phase after subarachnoid hemorrhage (SAH).

25 The prechiasmatic injection model was used, and 32 male Sprague–Dawley rats were divided into the sham-
26 operated, saline-injected (V group, ICP increase), and arterial blood-injected (SAH group, subarachnoid
27 blood plus ICP increase) groups. Morphological changes in cortical arteries and veins were observed
28 through the cranial window with a microscope before and up to 10 min after the injection. At 24 h, the
29 stenotic and obstructive cortical arteries and veins were counted. After 6 min, 60% of rats in the V group
30 showed vasodilatation, whereas all rats in the SAH group demonstrated vasodilation and/or
31 vasoconstriction (arterial instability) within 10 min. Similar acute venous congestive changes were
32 observed within 10 min in the V and SAH groups. At 24 h, stenotic and obstructive arteries and veins were
33 observed in the SAH group. Neurological deteriorations were observed at 1 h in the V and SAH groups,
34 and at 23 h in the SAH group. The sham-operated group showed no evident vascular changes and
35 neurological deterioration. The same phenomena, including arterial changes after 6 min and immediate
36 venous changes in the V and SAH groups, may have resulted from ICP increase, whereas subarachnoid
37 blood-related factors produced arterial instability within 5 min after blood injection. Subarachnoid blood
38 plays a significant role in hyperacute SAH pathophysiology in addition to ICP increase.

39

40 **Key words**

41 subarachnoid hemorrhage, hyperacute phase, arterial instability, venous congestion, vasospasm,
42 neurological finding, rat

43 **Introduction**

44 The prognosis of subarachnoid hemorrhage (SAH) is mainly determined by early brain injury (EBI) and
45 delayed cerebral ischemia. The former results from rapid intracranial pressure (ICP) increase by aneurysm
46 rupture and subsequent reduction of cerebral blood flow (CBF). Moreover, ICP-independent prolonged and
47 profound hypoperfusion are observed in the hyperacute phase after SAH, which result from peripheral
48 constriction of the microvasculature due to subarachnoid blood and bioactive substances [1,2]. As the
49 clinical outcome of SAH depends on patient severity on admission [3], early mechanism of brain damage,
50 particularly in the hyperacute phase, might provide a key role to overcome EBI to achieve favorable
51 outcomes.

52 Physiological cerebral circulation is controlled by suitable CBF from the major cerebral arteries to veins
53 and maintains brain homeostasis. However, the “vascular network” affects pathological changes at multiple
54 points in SAH [4]. Although morphological changes, such as microvascular constriction, play a role in
55 blood supply and cerebral autoregulation [5], there are limited reports evaluating the morphological changes
56 in the hyperacute phase after SAH [6]. Moreover, it is undetermined whether the morphological changes
57 are independently correlated with subarachnoid blood ICP increase. Therefore, we intended to evaluate the
58 specific pathophysiology, which was provided by subarachnoid blood plus ICP increase in addition to
59 morphological changes of cerebral vessels.

60 We aimed to observe the morphological changes in cerebral vessels in hyperacute phase after SAH by using
61 a rat model of prechiasmatic saline (ICP increase) and arterial blood (subarachnoid blood plus ICP increase)
62 injection.

63

64 **Methods**

65 *Animals*

66 All experimental procedures were performed in accordance with the Institutional Animal Care and Use
67 Committee of Kurume University. The procedures were conducted according to the National Institutes of
68 Health’s Guide for the Care and the Use of Laboratory Animals.

69 Thirty-two male Sprague–Dawley rats (Japan SLC, Shizuoka, Japan) weighing 310–346 g were randomly
70 divided into the sham-operated (S group, n=9), saline-injected (V group, n=9), and arterial blood-injected
71 (SAH group, n=14) groups.

72

73 ***Surgery***

74 Anesthesia was maintained with 2% isoflurane, and rectal temperature was maintained at $36\pm 0.5^{\circ}\text{C}$ with a
75 heating pad. SAH was induced using a prechiasmatic single blood injection method [7,8]. In brief, after the
76 tail artery of the rats was cannulated with a polyethylene catheter tube, a burr hole at the 7.5 mm anterior to
77 the bregma in the midline and a craniectomy window measuring 5×6 mm on their left hemisphere were
78 made using a drill. The rat was placed in a stereotaxic apparatus (Muromachi Kikai Co., Ltd., Tokyo, Japan).
79 A needle was tilted 30° caudally and lowered until the tip reached the skull base and placed at a site 1 mm
80 back from the base (11 mm below the surface). Fresh autologous blood (200 μL) was collected from the
81 tail catheter and infused over 12 s. In the V group, the same amount of saline was injected to the
82 prechiasmatic cistern in the same approach. In the S group, the needle was placed at the same position and
83 no solutions were injected.

84

85 ***Microscopic Observation***

86 Morphological changes in the cortical vessels were observed through the cranial window with a microscope
87 (SMZ800N; Nikon Solutions Co., Ltd., Tokyo, Japan). These changes were recorded using a digital camera
88 (MC170 HD; Leica Microsystems, Tokyo, Japan) before (pre-image) and up to 10 min after the injection.
89 As we intended to observe the vessels on the cortical surface after 24 h, we did not open the dura mater to
90 avoid drying and other mechanical injuries. After the skin was closed, the operative lesion was disinfected
91 with iodine, and a subcutaneous injection of meloxicam (1 mg/kg; Cayman Chemical, Ann Arbor, MI, USA)
92 was used for appropriate analgesia [9].

93

94 ***Image Analysis***

95 To assess the vessel diameter on the cortical surface, we reconstructed the image using ImageJ software
96 (National Institutes of Health, Bethesda, ML, USA) and monitored the dynamic changes for 10 min. Based
97 on the report by Wang et al. [10], we defined the arteries, which were observed on the cortical surface as
98 follows: primary arteries were main branches from the middle cerebral artery, secondary arteries from the
99 primary arteries, and terminal arteries from the secondary arteries (Fig. 1A, right). We selected the primary
100 or secondary arteries with the most evident changes every 2 min for 10 min. We measured the diameter and
101 then calculated the rate of changes in comparison with the vessel before the injection. We defined the vessel
102 changes as follows: none (less than 10% increase and decrease), vasodilatation (more than 10% increase),
103 and vasoconstriction (more than 10% decrease). In addition, we evaluated cortical venous congestion every
104 2 min for 10 min. We defined venous congestion when cortical vein showed “to and flow changes” or
105 “bluish changes.”

106 Although the photographs taken 24 h after the injection showed muddy dura mater, reddish changes on the
107 cortical surface and some vessel changes could be obviously found. Therefore, we counted
108 primary/secondary arteries and veins that represented more than 50% vasoconstriction (stenosis) and
109 obstruction, and calculated as follows: number of “the stenotic or obstructive vessels”/all vessel \times 100% in
110 each primary/secondary artery or vein.

111

112 *Neurological Findings and Brain Water Content*

113 Neurological scoring tests, including the Modified Garcia scale, beam walking, and rotarod tests were
114 performed in all groups at 1 and 23 h after the injection [9]. Then, anesthesia was maintained with 2%
115 isoflurane, and vessels were photographed on the cortical surface at 24 h. Subsequently, the rats were
116 decapitated, and the brains were quickly divided into the left hemisphere, cerebellum, and brain stem, and
117 weighed. They were incubated at 105°C for 72 h in an oven and measured the brain water content (BWC)
118 [9].

119

120 *Statistical Analysis*

121 We performed all measurements in a blinded manner. All data are presented as means±SEM, and statistical
122 analyses were evaluated using GraphPad Prism version 9 (GraphPad Software, San Diego, CA, USA) and
123 Ekuceru-Tokei 2019 statistical software (Social Survey Research Information Co. Ltd., Tokyo, Japan).
124 Parametric evaluations were performed using a one-way ANOVA with the Tukey–Kramer test in three
125 groups (BWT and RT and Garcia, BWC). Non-parametric analyses were performed using the Kruskal–
126 Wallis test, followed by the Steel–Dwass test among the three groups. Statistical significance was set at
127 $p<0.05$.

128

129 **Results**

130 *Mortality*

131 One rat in the sham group died from anesthesia complications, and the mortality rates in the vehicle and
132 SAH groups were 11.1% (one out of nine rats) and 35.7% (five out 14 rats), respectively.

133

134 *Image Analysis*

135 Image analysis was performed in six, five, and nine rats in the S, V, and SAH groups, respectively. No
136 changes in the cortical arteries were observed in the S group. After 6 min, three rats (60%) in the V group
137 showed vasodilatation, whereas all the rats in the SAH group demonstrated vasodilation and/or
138 vasoconstriction throughout the 10-min period (Fig. 1A, B). In contrast, acute venous congestive changes
139 were observed throughout the 10-min period in all rats of the V and SAH groups (Fig. 2).

140 Cerebrovascular appearance was clearly confirmed in seven, five, and six rats in the S, V, and SAH groups,
141 respectively, at 24 h. No stenotic vessels were observed in the S group (0%), whereas injured stenotic and
142 obstructive arteries were noted in the V ($17.6\pm 4.2\%$, $p<0.01$) and SAH ($40.7\pm 4.0\%$, $p<0.01$) groups; the
143 latter showed a significant increase ($p=0.03$, Fig. 3A). Injured vessels were observed in the S ($8.7\pm 4.4\%$),
144 V ($28.3\pm 6.1\%$), and SAH groups ($45.8\pm 5.2\%$), and the SAH group showed significant increase in rate in
145 comparison with the S group ($p=0.01$, Fig. 3B).

146

147 *Neurological Findings and Brain Edema*

148 Although the values of beam walking and rotarod tests at 1 h in the V (2.5 ± 0.2 , $p=0.02$; and 20.1 ± 7.7 s,
149 $p=0.03$; $n=8$, respectively) and SAH groups (1.7 ± 0.3 , $p<0.01$; and 12.5 ± 5.1 s, $p<0.01$; $n=9$, respectively)
150 were lower than those in the S group (2.5 ± 0.2 and 47.4 ± 5.3 s, $n=8$, respectively) (Fig. 4A, B). At 23 h post-
151 injection, no changes in neurological findings were observed in the V group ($n=8$) in comparison with the
152 S group ($n=8$) (3.1 ± 0.2 vs. 3.6 ± 0.2 in the beam walking test; 32.9 ± 6.9 vs. 67.7 ± 11.0 s in the rotarod test;
153 17.1 ± 0.2 vs. 17.4 ± 0.3 in the modified Garcia test). However, the values were significantly lower in the
154 SAH (1.6 ± 0.2 , 23.3 ± 8.3 s, and 14.7 ± 1.2 , respectively) than in the S ($p<0.01$, $p=0.03$, and $p=0.04$,
155 respectively) and V groups (beam walking; $p<0.01$) (Fig. 4C–E).

156 The BWC of the S ($n=8$), V ($n=8$), and SAH ($n=9$) groups in the left hemisphere, cerebellum, and brain
157 stem did not show significant differences (Fig. 4F–H).

158

159 **Discussion**

160 The strength of this study is the comparison of morphological phenotypes between ICP increase and
161 subarachnoid blood plus ICP increase. This study obtained the following novel findings. First, the SAH
162 group revealed arterial instability, including vasodilation and/or vasoconstriction in the first minute,
163 whereas the rats in the V group showed vasodilation slightly later than the saline-injected group. Second,
164 venous congestion was observed in the V and SAH groups in the first minutes. Finally, the cortical arteries
165 and veins represented significant stenotic and obstructive changes at 24 h after SAH.

166 Arterial instability, such as vasodilation and vasoconstriction, was immediately observed after SAH. This
167 phenomenon was continued throughout the 10-min period, whereas vasodilation was observed 6 min after
168 the injection. In hyperacute phase after SAH, several factors, such as platelet aggregation, basal lamina
169 degradation, and microvascular permeability, could contribute to the pathophysiology within minutes [11].
170 Further, exogenous materials in subarachnoid space and cerebrospinal fluid that originate from sudden
171 bleeding enhance EBI in SAH [2]. Therefore, in addition to ICP increase, those subarachnoid blood-related
172 factors may play a significant role on arterial instability in hyperacute SAH pathophysiology. The results

173 on hyperacute vasodilation were consistent with those of a previous study, which evaluated penetrating and
174 precapillary arterioles using different SAH rat models and reported that vasodilation was correlated with
175 reduction in CBF and velocity [6]. Vasodilation may present the compensatory mechanism for SAH-
176 induced CBF reduction. In contrast, the SAH rats in this study presented vasoconstriction, which was
177 reported to be observed at least 10 min in the experimental SAH model [12]. We did not assess further
178 detailed mechanism of the arterial instability. However, a previous *ex vivo* study showed biphasic responses
179 of vasodilation and vasoconstriction by electrical field stimulation in SAH arterioles [13]. The instability
180 phenotype might depend on the amount of subarachnoid blood, expansion manner, and individual arterial
181 condition.

182 Venous congestive changes were observed in both the V and SAH groups immediately after the injection.
183 According to papers on prechiasmatic blood injection model by Prunell et al. [7,8], ICP rapidly increases
184 and subsequently decreases within 5 min after blood/saline injection. However, the blood injection showed
185 more than 30% CBF reduction within 15 min, the saline injection instantly recovered within a few minutes.
186 The results suggest that the same phenomena, including arterial changes after 6 min and immediate venous
187 changes, in both the V and SAH groups, may have resulted from ICP increase, whereas subarachnoid blood-
188 related factors might produce arterial instability within 5 min after blood injection in this study. As
189 significant neurological deterioration at 1 h after the injection was similar between the V and SAH groups,
190 ICP increase might be more important to determine early neurological condition of patients with SAH.
191 Moreover, significant neurological deterioration at 23 h was observed in the SAH group. Therefore, SAH-
192 induced arterial instability and venous congestion observed in the hyperacute phase could be significantly
193 associated with SAH prognosis.

194 At 24 h post-injection, arterial stenotic/obstructive changes in the V group increased and were more evident
195 in the SAH group. Conversely, significant venous stenotic/obstructive changes were observed only in the
196 SAH group. Numerous vasoconstrictive factors were observed in SAH pathogenesis, and subarachnoid
197 blood obviously distributes brain parenchyma and participates in microvessel constriction and
198 microcirculatory deterioration [14]. As SAH pathophysiology also includes venous thrombosis [15],

199 subarachnoid blood-related vasoconstrictive factors in addition to ICP increase provide stenotic/obstructive
200 changes in arteries and veins.

201 In conclusion, although this observational study did not assess detailed mechanisms related to the
202 abovementioned results, we believe that the findings are helpful in understanding the SAH pathophysiology
203 in the hyperacute phase.

204 **References**

- 205 1. Schubert GA, Seiz M, Hegewald AA, Manville J, Thomé C. Hypoperfusion in the acute phase of
206 subarachnoid hemorrhage. *Acta Neurochir Suppl.* 2011;110:35–38.
- 207 2. Chen Y, Galea I, Macdonald RL, Wong GKC, Zhang JH. Rethinking the initial changes in subarachnoid
208 haemorrhage: Focusing on real-time metabolism during early brain injury. *EbioMedicine.* 2022;83:104223.
- 209 3. Connolly ES, Jr., Rabinstein AA, Carhuapoma JR, Derdeyn CP, Dion J, Higashida RT, et al. Guidelines
210 for the management of aneurysmal subarachnoid hemorrhage: a guideline for healthcare professionals from
211 the American Heart Association/american Stroke Association. *Stroke.* 2012;43:1711–1737.
- 212 4. Zhang JH. Vascular neural network in subarachnoid hemorrhage. *Transl Stroke Res.* 2014;5:423–428.
- 213 5. Lidington D, Wan H, Bolz SS. Cerebral Autoregulation in Subarachnoid Hemorrhage. *Front Neurol.*
214 2021;12:688362.
- 215 6. Ishikawa M, Kajimura M, Morikawa T, Tsukada K, Tsuji T, Kusaka G, et al. Cortical microcirculatory
216 disturbance in the super acute phase of subarachnoid hemorrhage - In vivo analysis using two-photon laser
217 scanning microscopy. *J Neurol Sci.* 2016;368:326–333.
- 218 7. Prunell GF, Mathiesen T, Svendgaard NA. A new experimental model in rats for study of the
219 pathophysiology of subarachnoid hemorrhage. *Neuroreport.* 2002;13:2553–2556.
- 220 8. Prunell GF, Mathiesen T, Diemer NH, Svendgaard NA. Experimental subarachnoid hemorrhage:
221 subarachnoid blood volume, mortality rate, neuronal death, cerebral blood flow, and perfusion pressure in
222 three different rat models. *Neurosurgery.* 2003;52:165–175
- 223 9. Takemoto Y, Hasegawa Y, Hayashi K, Cao C, Hamasaki T, Kawano T, et al. The Stabilization of central
224 sympathetic nerve activation by renal denervation prevents cerebral vasospasm after subarachnoid
225 hemorrhage in rats. *Transl Stroke Res.* 2020;11:528–540.
- 226 10. Wang KC, Tang SC, Lee JE, Tsai JC, Lai DM, Lin WC, et al. Impaired microcirculation after
227 subarachnoid hemorrhage in an in vivo animal model. *Sci Rep.* 2018;8:13315.
- 228 11. Sehba FA, Friedrich V. Early micro vascular changes after subarachnoid hemorrhage. *Acta Neurochir*
229 *Suppl.* 2011;110:49–55.

- 230 12. Sehba FA, Friedrich V, Jr., Makonnen G, Bederson JB. Acute cerebral vascular injury after subarachnoid
231 hemorrhage and its prevention by administration of a nitric oxide donor. *J Neurosurg.* 2007;106:321–329.
- 232 13. Koide M, Bonev AD, Nelson MT, Wellman GC. Subarachnoid blood converts neurally evoked
233 vasodilation to vasoconstriction in rat brain cortex. *Acta Neurochir Suppl.* 2013;115:167–171.
- 234 14. Li Q, Chen Y, Li B, Luo C, Zuo S, Liu X, et al. Hemoglobin induced NO/cGMP suppression deteriorate
235 microcirculation via pericyte phenotype transformation after subarachnoid hemorrhage in rats. *Sci Rep.*
236 2016;6:22070.
- 237 15. Zhang J, Peng K, Ye F, Koduri S, Hua Y, Keep RF, et al. Acute T2*-weighted magnetic resonance
238 imaging detectable cerebral thrombosis in a rat model of subarachnoid hemorrhage. *Transl Stroke Res.*
239 2022;13:188–196.
- 240
- 241
- 242
- 243
- 244
- 245
- 246
- 247
- 248
- 249
- 250
- 251
- 252
- 253
- 254
- 255

256 **Figure legends**

257 Fig. 1 Arterial instability in hyperacute phase after SAH.

258 (A) The left side indicates the changes in vascular diameter of cerebral arteries in each rat of all groups, and
259 the right side shows representative photographs and schematic illustration of the arteries on the cortical
260 surface within the cranial window.

261 (B) The left side shows temporal morphological changes in the cerebral arteries in each rat, and the right
262 side shows representative photographs of vasoconstriction and vasodilatation. The number of included
263 animals were six, five, and nine in the S, V, and SAH groups, respectively. Arrows and arrowheads indicate
264 vasoconstriction and vasodilatation, respectively.

265 pa, primary artery; sa, secondary artery; SAH, subarachnoid hemorrhage; ta, tertiary artery.

266

267 Fig. 2 Venous congestion in hyperacute phase after SAH. The left side shows the congestive changes in the
268 veins in each rat of all groups, and the right side shows representative photographs of the changes. The
269 number of included animals were six, five, and nine in the S, V, and SAH groups, respectively. Arrowheads
270 indicate bluish veins.

271 SAH, subarachnoid hemorrhage.

272

273 Fig. 3 Stenotic and obstructive changes in arteries and veins at 24 h after SAH.

274 (A) stenotic and obstructive changes in cerebral arteries at 24 h after the injection in the S (n=7), V (n=5),
275 and SAH (n=6) groups.

276 (B) Stenotic and obstructive changes in cerebral veins at 24 h after the injection in the S (n=7), V (n=5),
277 and SAH (n=6) groups. Arrows and arrowheads indicate stenotic change in cerebral artery and stenotic and
278 obstructive changes in veins, respectively.

279 a, artery; SAH, subarachnoid hemorrhage; v, vein.

280 *, $p < 0.05$.

281

282 Fig. 4 Neurofunction and brain edema at 24 h after SAH.
283 Neurofunction of beam walking (A) and rotarod (B) tests at 1 h, and beam walking (C), rotarod (D), and
284 modified Garcia (E) tests at 23 h post-injection. Brain water content in the left hemisphere (F), cerebellum
285 (G), and brainstem (H) at 24 h post-injection. The number of included animals were eight, eight, and nine
286 in the S, V, and SAH groups, respectively.
287 SAH, subarachnoid hemorrhage.
288 *, $p < 0.05$.

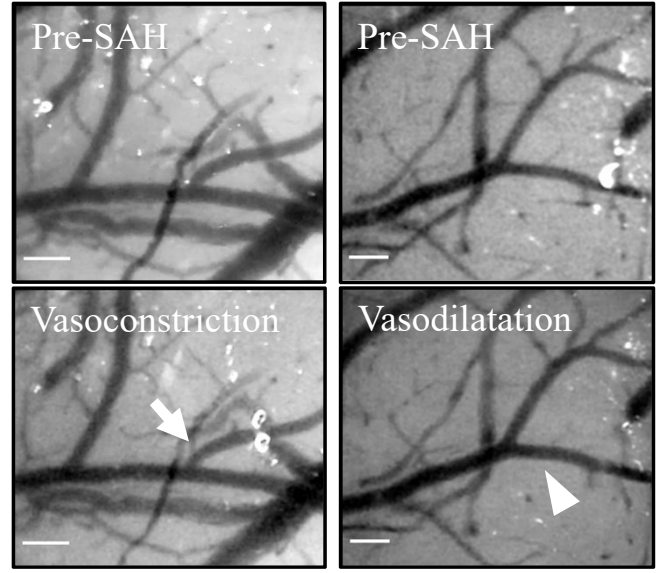
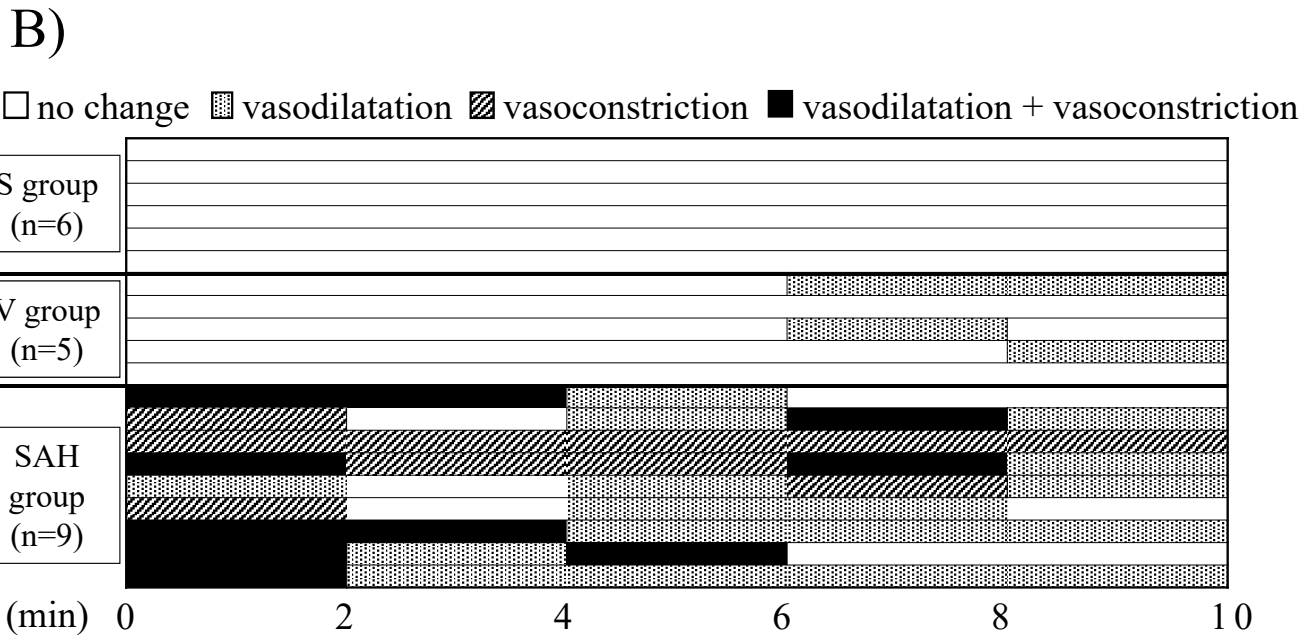
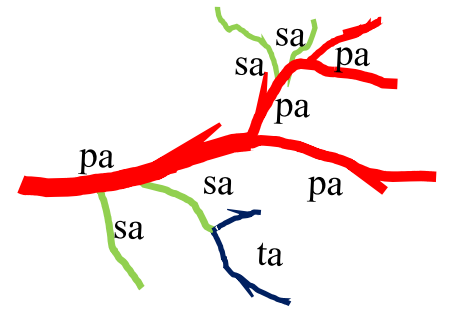
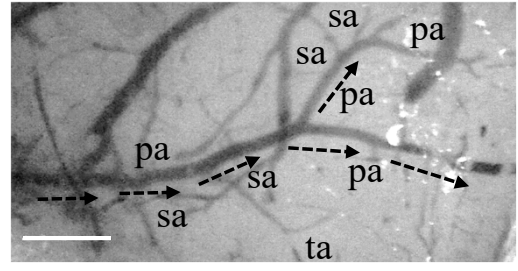
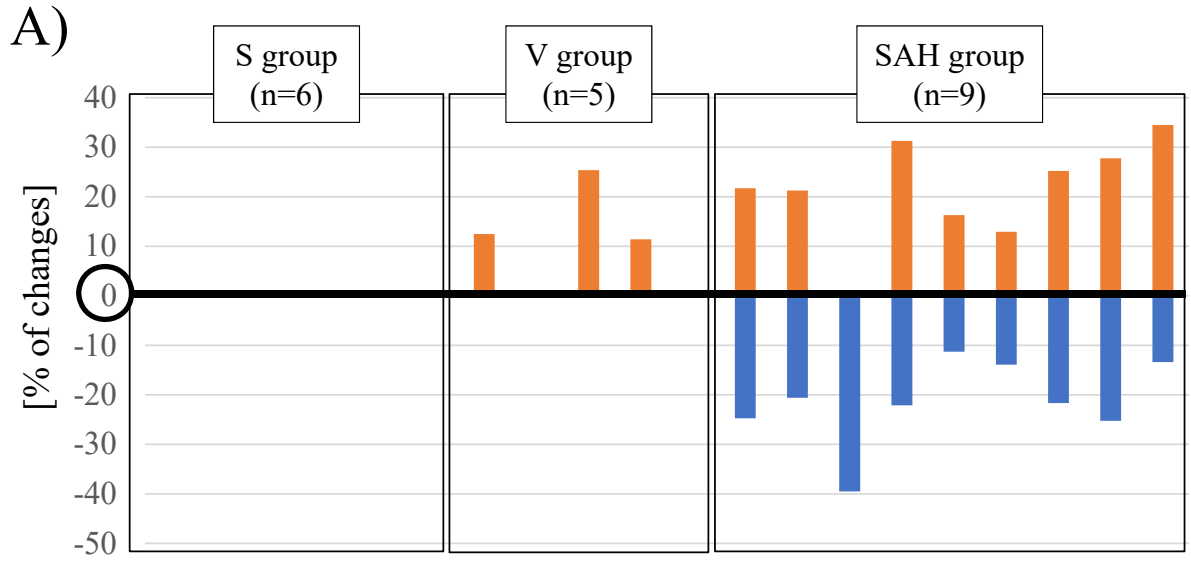


Fig.1

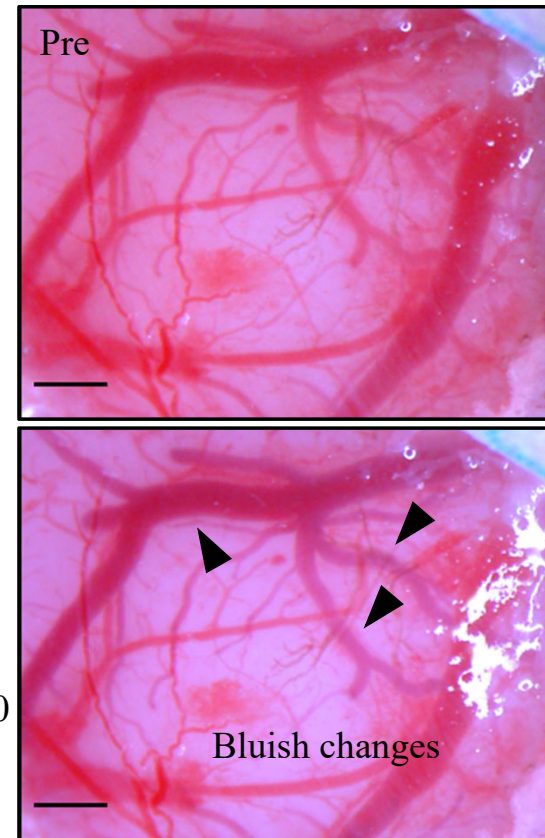
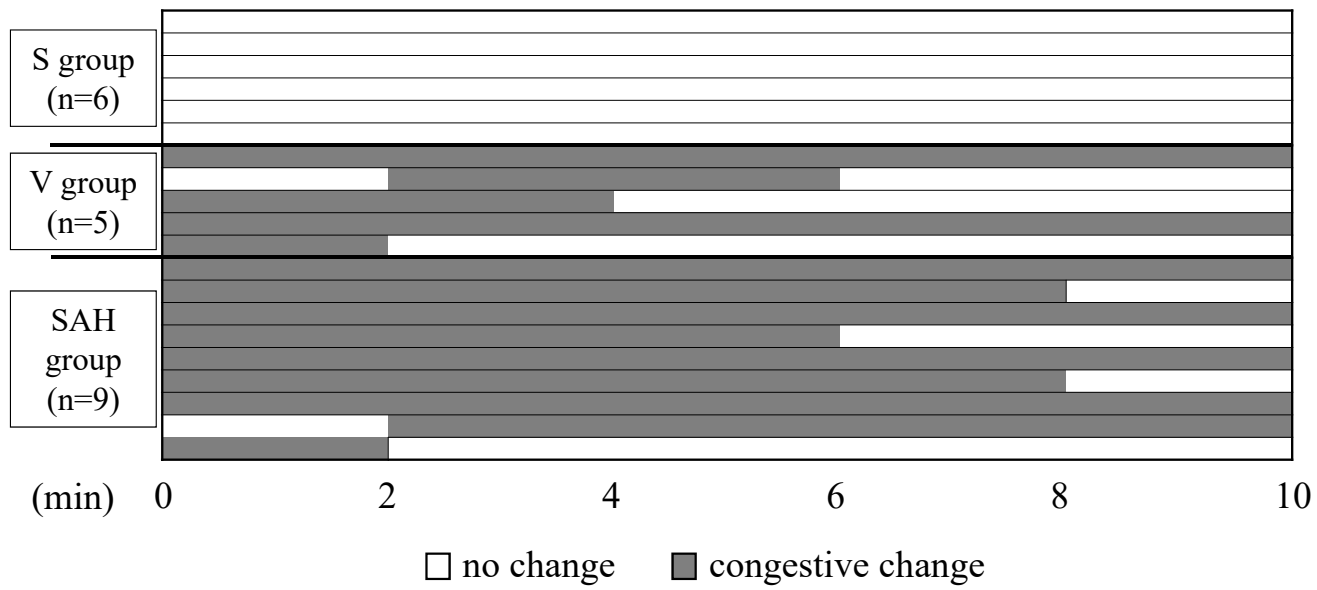
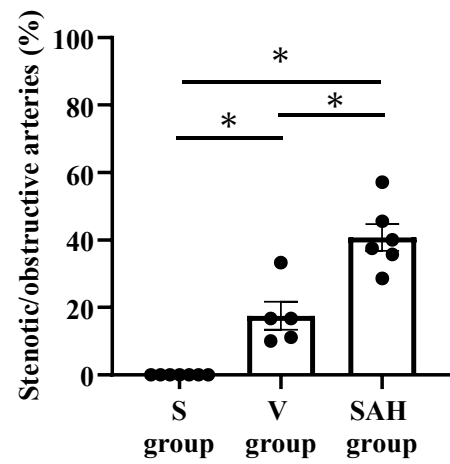


Fig.2

A) Arteries



B) Veins

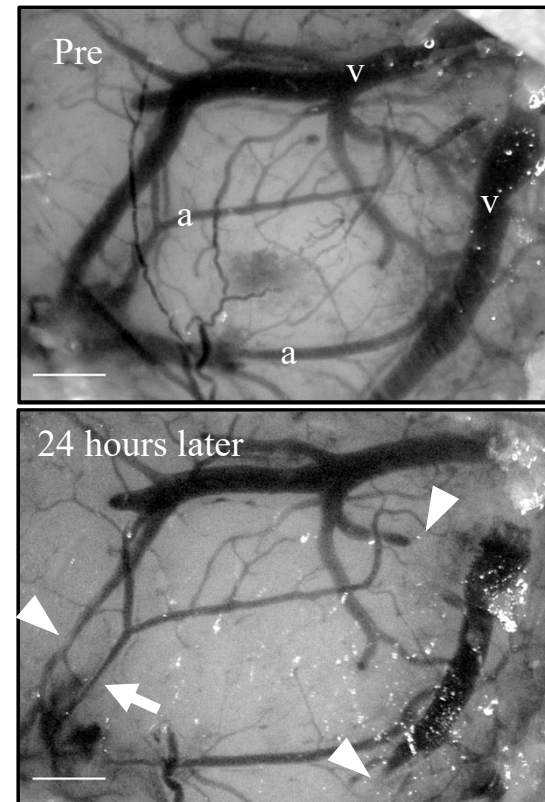
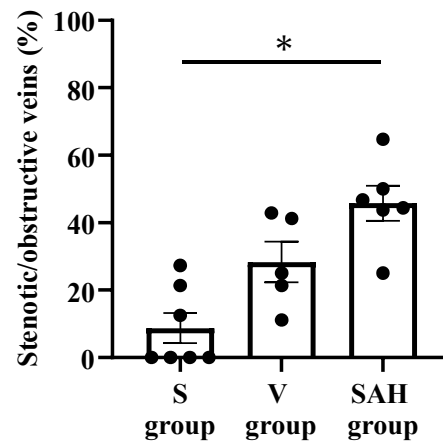


Fig.3

